NPL

National Physical Laboratory

Good Practice Guide No. 152

The use of EBSD for analysis of additively manufactured materials

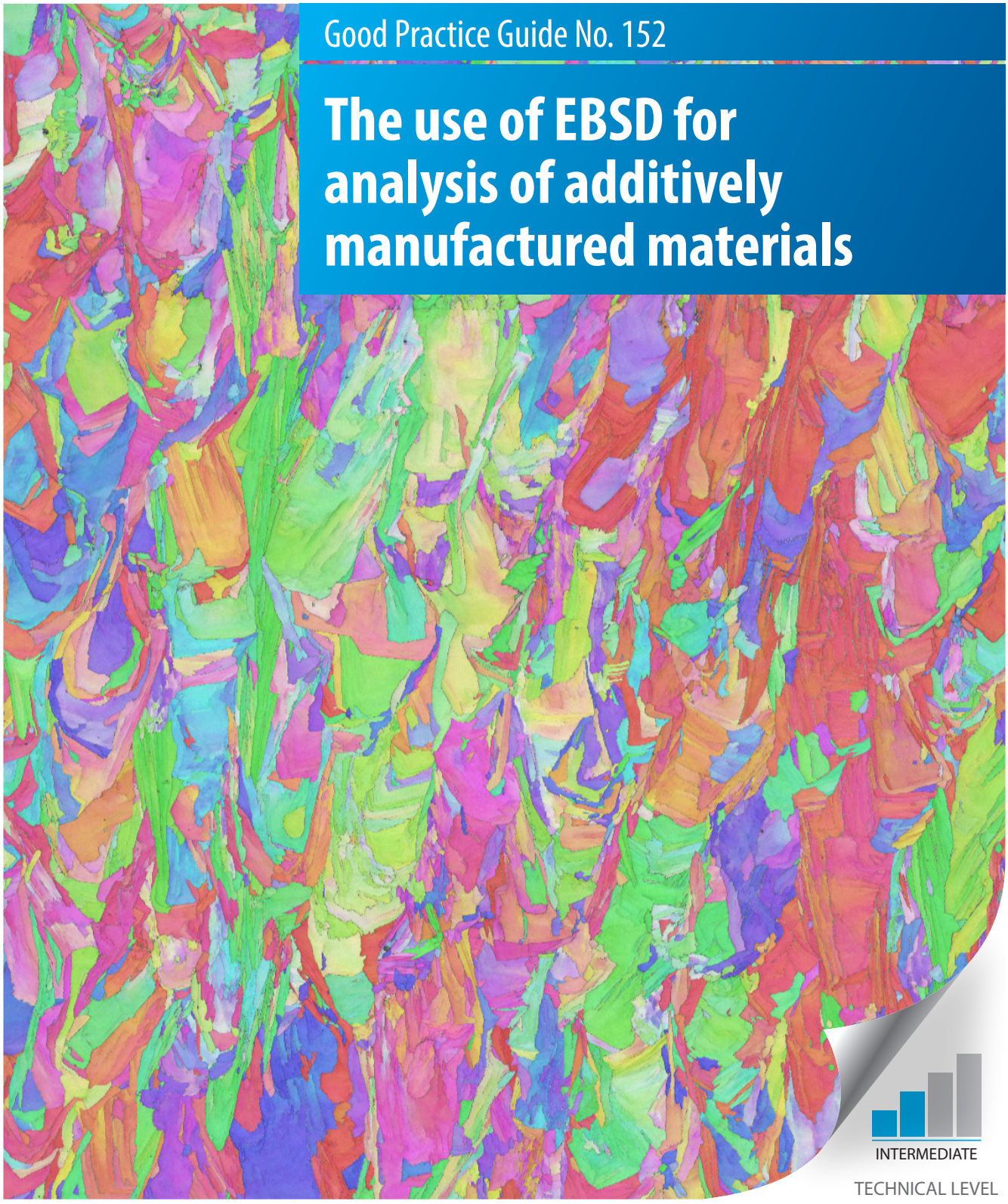

INTERMEDIATE

TECHNICAL LEVEL

Department for Business, Energy & Industrial Strategy

FUNDED BY BEIS

The National Physical Laboratory (NPL)

NPL is the UK's National Measurement Institute, and is a world-leading centre of excellence in developing and applying the most accurate measurement standards, science and technology available.

NPL's mission is to provide the measurement capability that underpins the UK's prosperity and quality of life.

Version 1.0

https://doi.org/10.47120/npl.mgpg152

NPL Authors and Contributors

K.P. Mingard

Find out more about NPL measurement training at **www.npl.co.uk/training** or our e-learning Training Programme at **www.npl.co.uk/e-learning**

National Physical Laboratory
Hampton Road
Teddington
Middlesex
TW11 0LW

Telephone: +44 (0)20 8977 3222
e-mail: training@npl.co.uk
www.npl.co.uk

Guide information

What is it about?

A wealth of information on the structure of materials made by additive manufacturing (AM) processes can be obtained by Electron Backscatter Diffraction (EBSD) mapping of polished sections. Data such as the size, shape and orientation of the grains and their distribution can be obtained, and when quantified reveals information on the manufacturing process or can be related to the physical properties of the components produced. Using EBSD datasets acquired from AM produced Ni-base superalloys, multiple examples are used to illustrate the information available and to show how spatial variation can be easily represented. Particular attention is paid to ensuring that useful and reliable comparisons between datasets can be produced.

Who is it for?

This guide is aimed particularly at producers and users of AM materials or students relatively new to the subject and looks to demonstrate the range of information that can be derived from EBSD maps.

What is its purpose?

The guide aims to ensure the data acquired is quantified and reported in a manner that allows comparison with other EBSD datasets. The wrong choice of EBSD acquisition conditions or parameters to plot can result in erroneous conclusions, based on noisy or restricted, and therefore unrepresentative, data sets. It emphasises where care is needed in reporting data, for example because the definitions for calculation of the value of a particular parameter vary between software packages. EBSD maps can also lead to misleading comparisons because, for example, the map colour scale is not defined fully. Using EBSD datasets acquired from AM produced Ni-base superalloys multiple examples are used to illustrate the issues above and to show how spatial variation can be easily represented

What is the prerequisite knowledge?

The guide can be read by someone unfamiliar with the actual acquisition or processing of EBSD data but it does assume a basic understanding of the microstructure and features such as grain structure that might be of interest in an AM metal. It gives details that a user of EBSD processing software could apply to produce reliable data, without assuming the use of specific EBSD operating software.

Acknowledgements

This work was funded by the National Measurement System run by the UK Government Department for Business, Energy and Industrial Strategy.

The samples analysed were provided by Anand Kulkarni, Siemens Corporation, and Caitlin Green is thanked for sectioning and polishing the samples for examination.

Rene de Kloe from Ametek EDAX is gratefully acknowledged for mapping of the large area cross section used throughout this guide.

Contents

This page was intentionally left blank

Chapter 1

Introduction

Electron Backscatter Diffraction (EBSD) is frequently used to characterise Additively Manufactured (AM) materials. EBSD data contains a wealth of information on the size, shape and orientation of the grains resulting from the melting and solidification of, or sintering after debinding of, the powder layers deposited during the manufacturing process. The data can reveal information on the manufacturing process or can be related to the physical properties of the components produced. It has been used to understand the detail of the microstructural evolution during solidification [1,2], and extended to the 3D evolution of structure and orientation [3,4]. More generally EBSD maps are frequently shown to illustrate the overall microstructure of the AM material under examination, complementing a range of other microscopy techniques e.g. [5-7].

A significant advantage of the EBSD technique is that the data generated can be quantified to enable correlation between:

a) Changes in microstructure between different locations in the component, revealing variation of, for example, heat flow and thus solidification rates

b) Changes in microstructure between parts, suggesting variation manufacturing conditions from, again for example, inconsistent powder layer deposition

c) Final component properties and the structure which in turn feeds back into control of, or changes to, the manufacturing process

Even without quantification, EBSD maps can help with visualisation of the processes going on during manufacture, but this still necessitates an understanding of how best to plot maps and choose the correct parameters and scales with which to produce the maps, or figures to illustrate preferred crystal orientations. The wrong choice of EBSD acquisition conditions or parameters to plot can result in erroneous conclusions, based on noisy or restricted and therefore unrepresentative data sets.

This guide covers some of the basic aspects to consider when using EBSD to map an AM sample. Firstly, it aims to illustrate some of the range of information that can be derived from EBSD maps, and secondly and most importantly aims to ensure the data acquired is quantified and reported in a manner that allows comparison with other EBSD datasets. Modern commercially available EBSD software can generate maps and data very simply, but if the details are not considered for how the software makes and reports measurements, invalid comparisons can result. This can occur, for example, because different software programs use different definitions for calculation of the value of a particular parameter, or because default parameters are changed without realising, or frequently because the map colour scale is not defined fully.

The guide is aimed more at producers and users of AM materials or students relatively new to the subject with limited familiarity with the operation of EBSD systems. It is not a guide to sample preparation or operation of EBSD systems, apart from where the operation impinges on acquiring a useful dataset that is sufficiently representative to answer the questions being asked about the process or sample. For more general information on the use of EBSD there are a range of introductions to the technique including EBSD system suppliers websites, YouTube videos [8] or published texts [9].

The range of AM materials and production conditions is extremely large, so the guide cannot be fully comprehensive for every material type, so it concentrates on one of the alloy types, Ni-base superalloys, which is a commonly produced material that is representative of many of the issues encountered.

This page was intentionally left blank

Chapter 2

Preferred orientations and relationships to sample geometry

2.1 Sample location and definition

The majority of AM materials are produced by deposition of powder layers and progressive/ repeated sintering or melting of these layers between deposition by, for example, scanned laser or electron beams. Therefore, in general the resulting microstructure will show a strong relationship to the growth (Z) direction, perpendicular to the layers, and potentially also in the orthogonal XY plane where X and Y are defined either by the sample geometry or the scan pattern of the beam and its relationship to the sample geometry.

It is essential therefore that preparation of samples for polishing and EBSD examination can be related to the three axes. This is often overlooked when samples are prepared from components with a circular cross section (Figure 1). If the axis of such a sample is in the growth (Z) direction, the X-Y scan orientation can be lost if this is not noted before removal from the AM machine. Figure 2 shows an example map of an X-Y plane in which there is clear alignment of many of the grains, but it was not recorded how the axes the alignment might define relate to the equipment axes or to the scan profile. Alternatively, if a cylinder (such as a tensile specimen) is grown, or machined from a sample grown with the axis parallel to the powder bed, the orientation of Z relative to a cross section may also be lost. If the original sintered surface is retained, the axes may be deduced from the surface appearance.

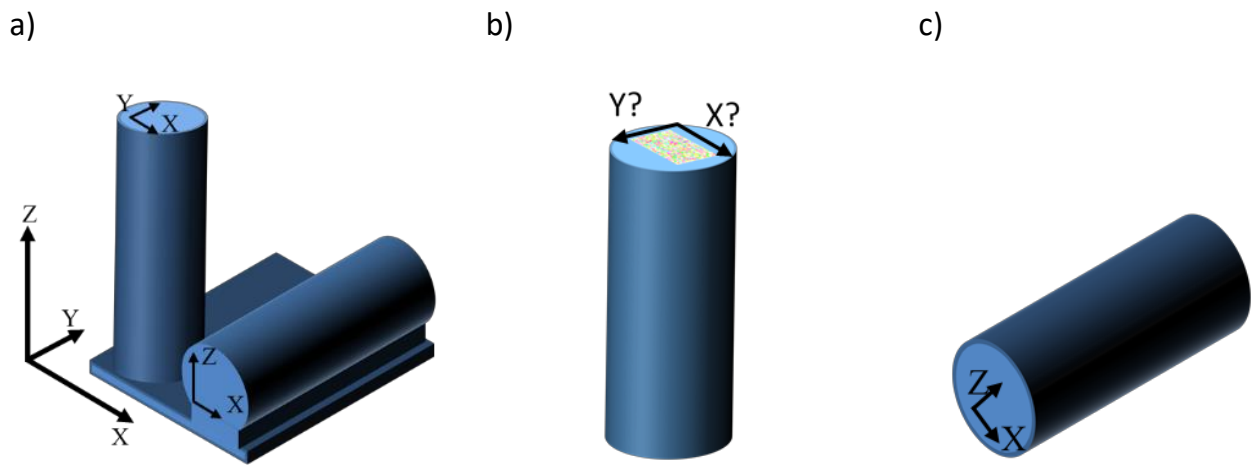

Figure 1. *a) As-built AM structures to produce cylinders for tensile testing parallel and perpendicular to the growth direction Z. b) Parallel growth cylinder removed from base and machined in o.d. with no obvious relationship to original X and Y or beam scan axis. c) Similarly cylinder machined from perpendicular growth direction with no obvious orientation relationship to X-z axes.*

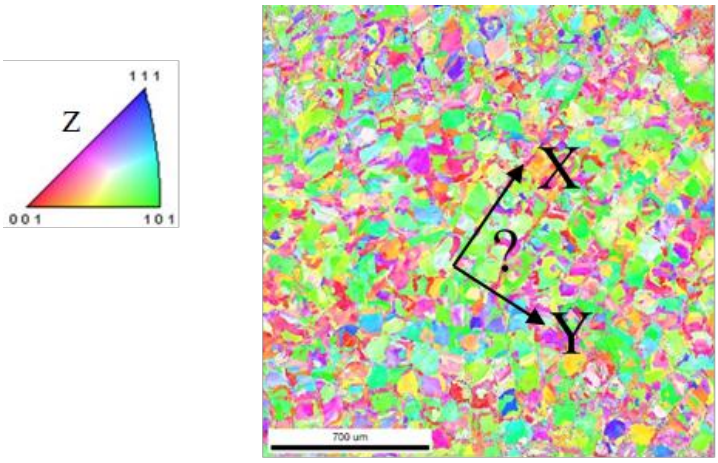

Figure 2. *IPF(z) orientation map of a section perpendicular to the Z growth direction of cylindrical sample of a Ni superalloy in which the orientation relative to the AM X and Y axes has been lost, so the repeating structure cannot be related to the scan used.*

2.2 Texture – crystallographic orientations relative to growth directions

The crystallographic texture, or preferred orientation, of a material affects its anisotropic properties, including stiffness, mechanical strength, and electrical resistivity. In AM manufactured materials, texture depends on the build axes and can be controlled by tuning the build parameters.

2.2.1 Sample- microscope orientation relationships

Even if the relationship between the AM manufacturing X-Y-Z axes and the cross-section polished for EBSD are known, a further alignment of axes needs to be understood when the EBSD map is acquired. Figure 3a shows a map of Ni superalloy in which the grain elongation clearly indicates the AM Z axis growth direction is vertical, but whether it is upwards or downwards is less obvious. Depending on the relationship between the SEM sample tilt axis, scanning axes and EBSD detector, the “top” of the sample when tilted may appear at the bottom of the map(or even rotated 90° in some microscopes). Figures 3b and c show this schematically for a cross section taken from the horizontal semi-cylindrical sample shown in Figure 1a in which the tilted sample appears mapped upside down. A calibration method to determine the relationship between sample, microscope and EBSD system axes may be found in [10].

The relationship between the SEM-EBSD axes and the sample becomes even more important when texture is to be analysed.

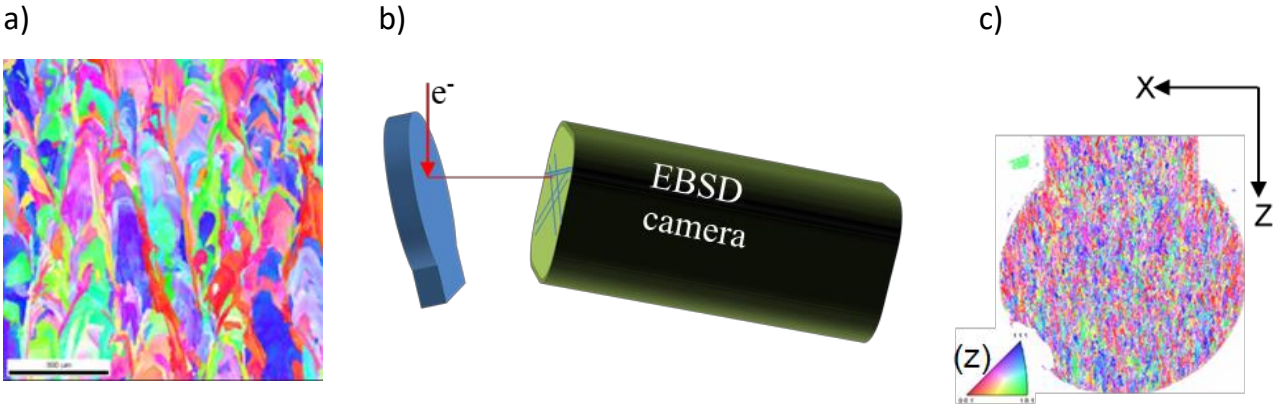

Figure 3. *a) example of an IPF(z) orientation map of a section from a sample in which it is not obvious if the AM (Z) growth direction was up or down. b) Orientation of a sample in the SEM relative to the electron beam and EBSD camera and c) the map that could result from the orientation in b).*

2.2.2 Sample Texture – orientation colour scale maps

The maps in Figures 3a and 3c use what is often the default orientation colour scale based on an inverse pole figure, in which the colour is determined by the crystallographic direction or plane normal to the plane of the mapped surface. For the illustrated case of a material with cubic symmetry, the orientations will all fall within the portion of the stereographic projection shown. Depending on the software used, this colour scale normal to the plane may be referred to as IPF(z) or IPF[001], the former potentially confusing for AM as this EBSD Z axis may well not be the same as the AM growth direction.

If only the default IPF scale is used, then it is possible that important information may be missed. In the examples in Figure 3, the grain orientations normal to this plane appear to be randomly distributed. However, if the orientations are viewed from directions within the plane of the map/sample, then a different picture emerges. Figure 4 shows IPF colour scale maps for the three orthogonal directions on the sample (now oriented so that the AM growth direction is vertically upward in the plane of the maps). The predominance of green hues in Figure 4c show there is a preferred <101> orientation in the direction of growth, but with no preferential rotation about this axis. Additionally Figure 4c makes a change in preferred orientation more visible at the outer edges of the sample above the level at which the sample diameter increases to a preferred orientation. An increase in red colour in these regions shows a tendency towards the red/cubic <100> aligned with the growth direction; a change in this region was just about visible in the IPF(z) map of Figure 4a but was less prominent and more difficult to interpret.

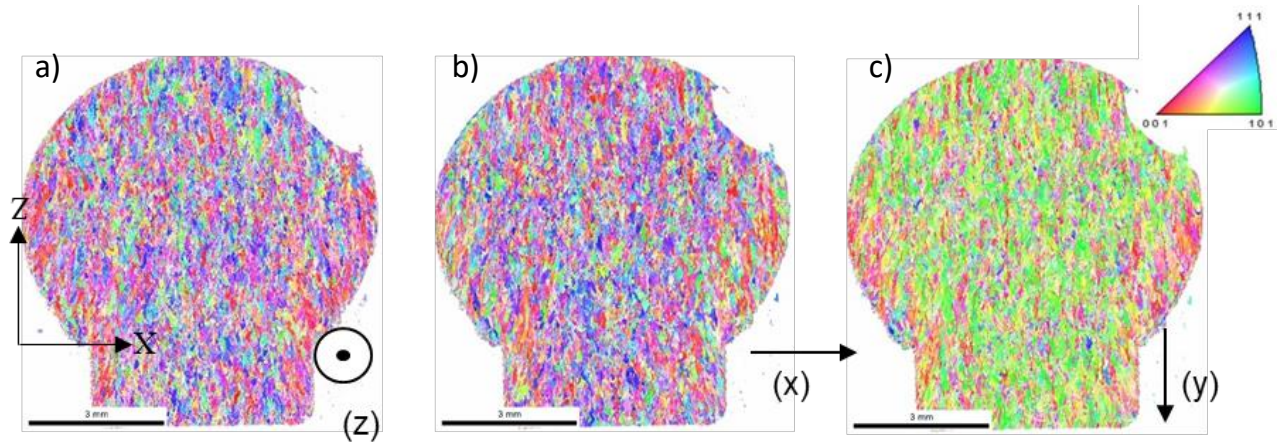

Figure 4. *Three IPF orientation colour maps in which the colour scale is derived from the orientations aligned a) perpendicular to the plane (IPF(z) or IPF (001) , b) horizontally (IPF (x) or IPF (100) and c) vertically (IPF(y) or IPF (010). Note that the AM build axes Z and X are vertical and horizontal.*

2.2.3 Pole and Inverse Pole Figure plots

Quantification of preferential orientations such as that seen in Figure 4 can be obtained by plotting of pole figures and inverse pole figures. Similarly to inverse pole figure maps, an inverse pole figure shows the crystal directions pointing along a specified sample axis. But instead of plotting the directions as colours on a spatial map, the directions can instead be plotted on a spherical scatter plot, where the sphere radius points along the plotted crystal directions. Since crystals are symmetric – for example, a cubic crystal has 24-fold rotational symmetry – the sphere can be reduced to a 1/24th segment ('the fundamental zone') usually shown as a triangle (Figure 5). Spatial information about the measured orientation is lost, but the relative distribution of all crystal orientations relative to a single sample axis can be quantified. Standard EBSD software can convert the scattered points into an orientation density function, which can be displayed as a contour map such as that shown below in Figure 5a for the whole of the sample seen in Figure 4; the colour scale shows the density relative to that expected from a random distribution of orientations. Similarly, pole figures show the distribution of a single crystal orientation relative to the sample axes. Figure 5b shows pole figures for the three principal crystal axes for the sample. The <101> alignment noted in Figure 4c is reflected by the highest values at the [101] apex of the [100]/(x) IPF map and top and bottom of the vertical axis for the [101] pole figure.

However, there are multiple possible methods for calculating the density distribution (e.g. harmonic series expansion or discrete binning in EDAX-TSL software), and parameters such as the Gaussian half width that smooths the data can be varied significantly (in value and, between software programs, by definition (half or full width). The colour scale

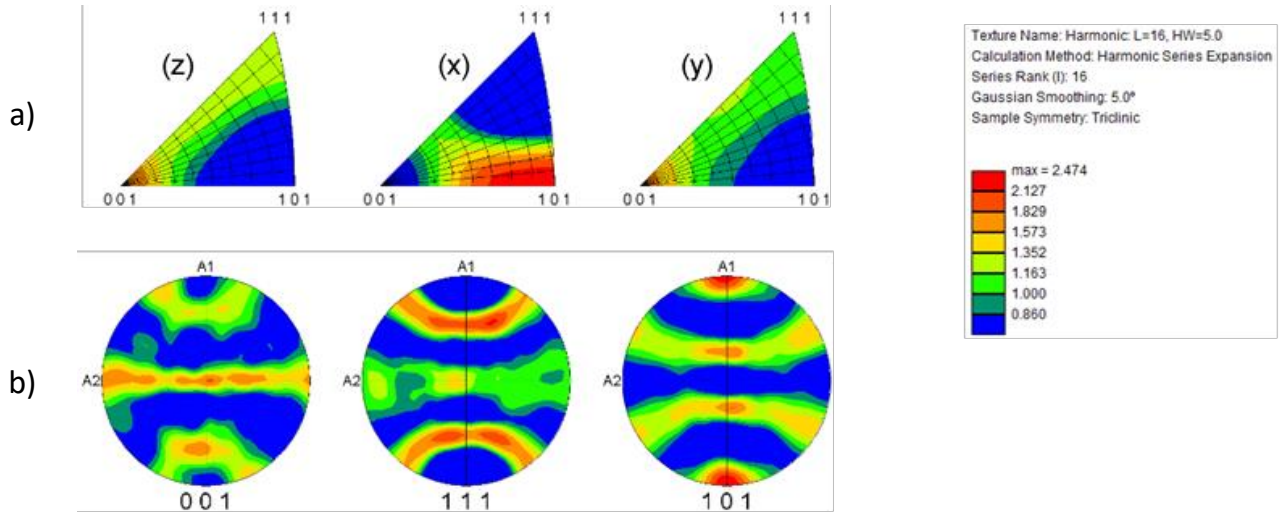

Figure 5. *Top row a): Inverse Pole Figure plots for the 3 axes indicated for the mapped region shown in Figure 4 and b. Bottom row b): Pole Figure plots to show the orientations of the {001}, {111} and {010} plane normals relative to the plane of the page. Note the key to the plots gives details of the plot calculation methods and colour scale relative to the maximum 2.5x multiple of a random deviation.*

(log/linear/discrete/continuous) can also be altered (Section 4 has more details on this) so if comparisons of the texture intensity are to be drawn between pole figures, care must be taken with the colour scale. The maximum in the above example could be reduced from ≈2.5 to 2.0 by changing to discrete binning although only subtle differences in spatial distribution would be seen in the plots. There is also a tendency to scale to the maximum value, and this can often over-emphasise the texture intensity for low values (typically <2) or suggest equivalence when the scales are actually very different.

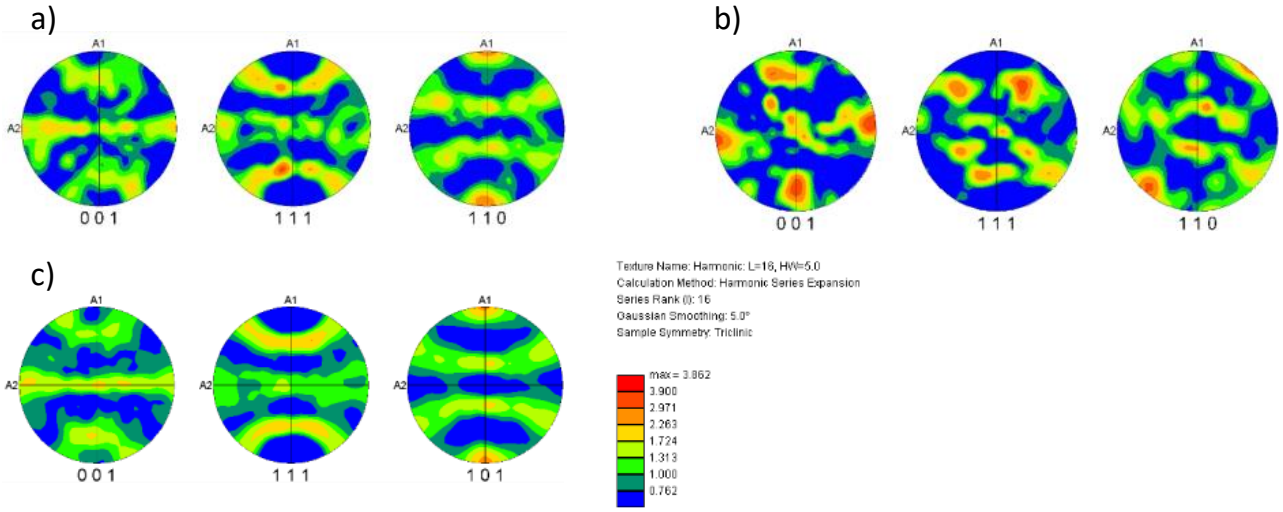

Figure 6. *Pole figure plots to show differences in preferred orientation at a) the vertical centre line of the sample in Figure 4, b) the segment below the horizontal diameter where the diameter expands outwards from the base and c) the overall preferred orientations of the sample, reproducing Figure 5 on the new colour scale.*

If more detailed understanding or quantification of texture is needed, then consideration should be given to measurements from sub-sections of the mapped area. For the sample shown in Figures 3 and 4, Figure 6 shows pole figures from the vertical centre line (the area approximately 1 mm either side of the centre) and from a segment below the horizontal diameter where the diameter expands outwards from the base. The switch between [101] and [001] alignment is clear, and the maximum scale value is now 3.9 compared with 2.5 previously.

A final consideration for this section is to utilise the information in the (inverse) pole figures to replot maps, by creating subsets of data to show grains with a particular orientation. Figure 7a-c) shows those grains with respectively [001], [111] and [101] orientations within 15 degrees of the normal to the plane; in this example the change in preferred orientation at the outer edges of the sample is highlighted. It can sometime be useful to compare these with maps of other grain properties, discussed in the following section.

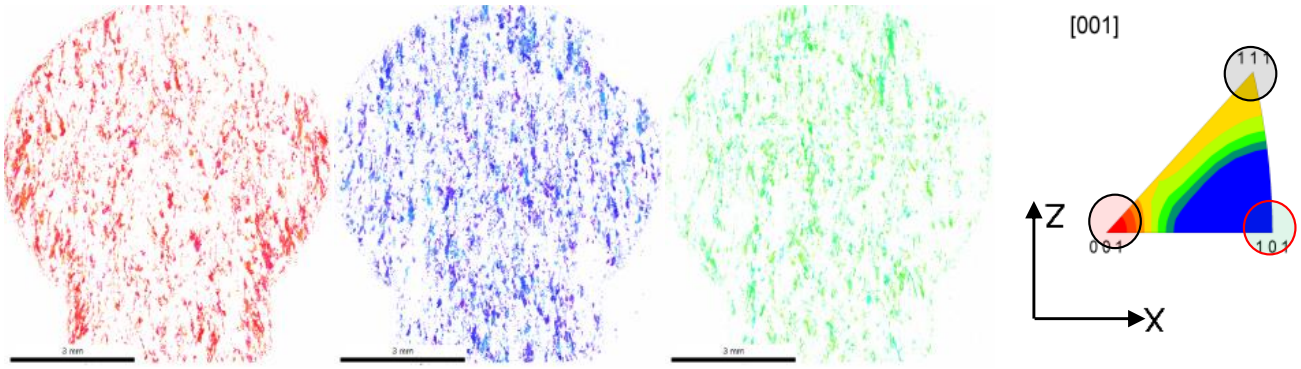

***Figure 7**. Subsets of the IPF (z) orientation colour scale maps showing the position of grains with orientations a) {001} b) {111} and c) {101} within 15° of the plane normal.*

The preceding examples just highlight a few aspects to consider, for a simple cubic structure. For other crystal structures and more detailed analysis and interpretation more information can be found in, for example, [11,12].

2.2.4 Comparison of Different Sections

It should also be obvious that conclusions about texture from maps of one plane should be confirmed and indeed extended by examining the texture of planes perpendicular to it. Thus in the preceding examples, the alignment of <101> in the growth direction is confirmed by the bias towards the green [011] of the IPF colour scale in the plane normal section of Figure 2. A second section may also reveal banding in the structure, which may indicate the need for a second primary section through a different point in the banding.

2.3 Summary

- Record sample orientation with respect to the AM manufacturing axes
    - Especially when circular cross sections
- Understand SEM/EBSD map orientation wrt sample axes
    - Plot the sample axes on maps
    - Don’t just plot the default IPF Z orientation map
    - Don’t confuse IPF and AM axis labels
- Understand the different options open for map plotting
    - Plot IPF orientation colour scale maps for 3 orthogonal axes
- Consider plotting subsets – maps of regions of the pole figures or pole figures from regions
- Use a consistent colour scale on PF an IPF and ensure the maximum value is recorded to allow comparisons
- Map orthogonal planes

Chapter 3

Measurement of grain size and shape variation

Measurement of grain size and shape is a complex subject made more difficult in many AM materials by material anisotropy, with elongation of grains often observed in the direction of solidification, sometimes with periodic variation resulting from melting and remelting and the beam scan pattern. As the previous example showed, preferentially oriented grains can grow at the expense of others, resulting in a wide or even bimodal size distribution. A single mean grain size value can be meaningless, and certainly the way in which a mean value is calculated is important if it is to be used to compare samples. The same considerations apply to (mean) values of shape factors such as aspect ratio.

Discussion of the appropriate mapping conditions such as step size (defining the map pixel size), minimum mapped area and grain boundary definition (10° misorientation is used in the following) are covered in detail elsewhere (e.g. ISO 13067 [13]). However, in the context of AM materials there are two extra considerations worth noting here:

a) The microstructure of many AM materials can vary with position in the build, often as solidification conditions change with geometry, and mapping by EBSD will need to take this into account, either by mapping the whole of a cross section, or by selection of representative areas of that cross section.

b) In the case of individual representative areas, care must be taken where elongated grains are present that a sufficiently large area is mapped.

3.1 Mapping representative areas

The maps in Figure 4 are a good example of mapping of the whole cross section, revealing variation from edge to centre and at changes in geometry, and analysis of the variation in grain structure will be considered later in this section.

Time or equipment may however mean that this extensive mapping is not possible and instead maps of smaller regions will be obtained. The maps of these regions must contain a sufficient number of grains that are fully within the map as the grain elongation makes it impossible for any accurate estimate of true size for partially mapped grains touching the map edges.

Figure 8 shows 3 maps acquired from the centre of the sample described in Figure 3-7. They cover different areas, with all grains shown (Figures 8a-c) and without grains touching the edge (Figures 8d-f). (Note that they are not shown to the same scale). Figure 8d shows that a significant fraction of the grains of Figure 8a touch the edge and it is clearly too small an area for accurate measurements since the large grains have a higher probability of touching an edge and being excluded. This judgement is more difficult to make for Figure 8b, but Figure 8c clearly covers an area large enough with most grains fully within the mapped area.

It is also worth noting in passing that the map pixel sizes are 1, 2 and 2.5 µm, so the smallest grains that were measured with reasonable accuracy (10 pixels area or more) are 3.3, 6.6 and

8.3 µm circle equivalent diameter (for a hexagonal grid). The total number of grains measured in each image were 766, 601 and 2822. The reason more grains were measured in Figure 8a than 8b is mostly the function of the smaller step size, which resulted in measuring 395 grains < 5 µm (dceq) in Figure 8a and only 101 in Figure 8b. A poor surface quality for figure 8a may also account for more smaller grains.

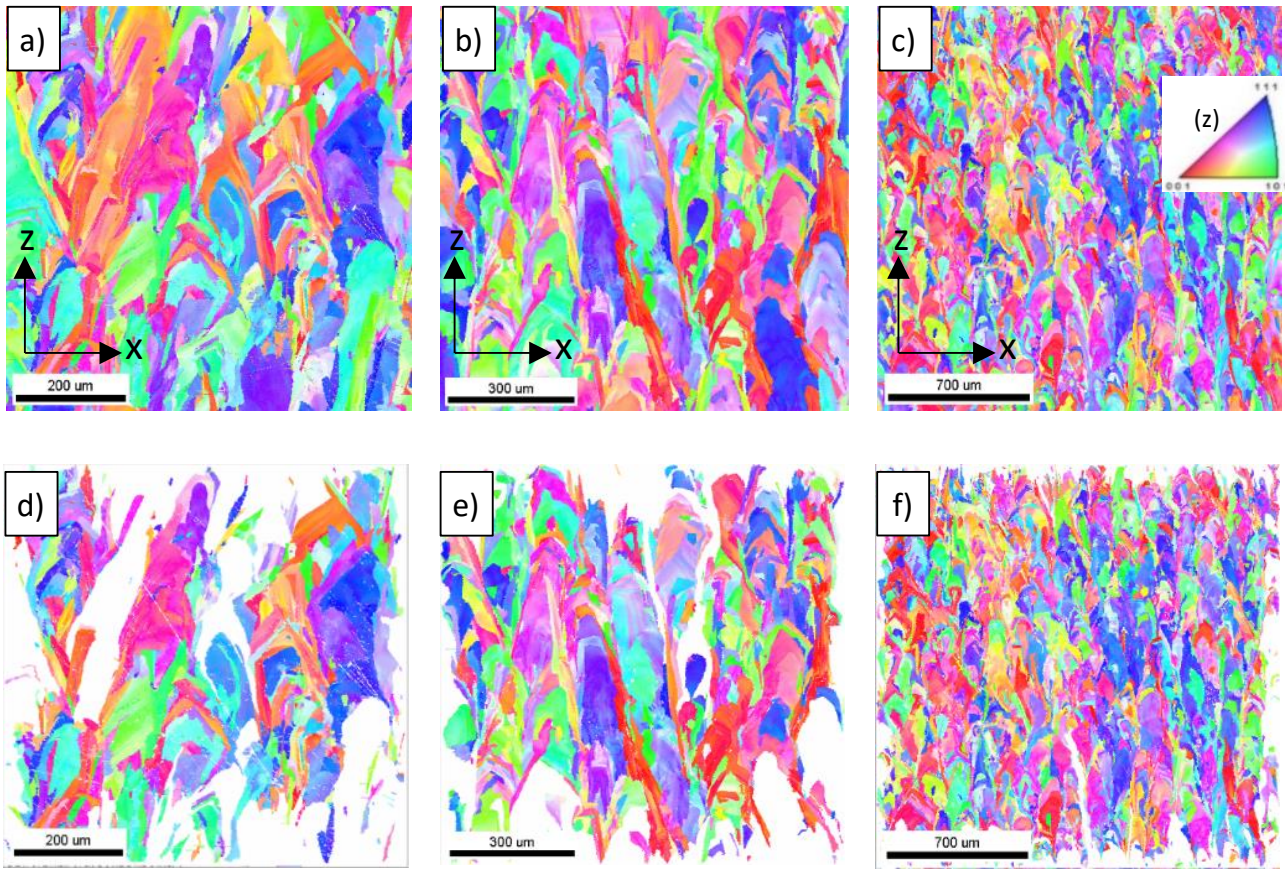

Figure 8. *Maps of the same polished face of an AM Ni superalloy acquired from areas of a) 0.54 mm², b) 0.94 mm² and c) 4.00 mm², with step sizes of 1, 2 and 2.5 µm respectively. Figures 2 d), e) and f) show the same maps with all grains touching the map edges removed. (Note the AM deposition axes are shown for each map).*

3.1.1 Mapping large areas

To map the large areas needed to see a representative area of a sample it can be tempting to simply reduce the magnification on the SEM until the field of view is, for example,1 mm or even 2 mm. With a large enough step size this area can be mapped in a short time. If possible, this should be avoided for the following reasons:

i) Inherent in the SEM scanning of a tilted sample are trapezoidal distortions which, while always present, increase rapidly as the field of view is widened below 500 µm [14]. Sample misalignments or inaccurate tilts can add to the above and mean that deviations from reported linear dimensions can vary from 0 to 10% with position on the map.

ii) Adjustment of the focus correction ("dynamic focus") needed for the changing sample working distance becomes more critical to obtain sharp EBSPs rather than diffuse patterns from a defocused beam spread over several grains

iii) The correction for beam deflection of the EBSD pattern centre will become less accurate and lead to more mis-indexing

If possible, a large area should be mapped with automated routines that stitch together multiple smaller maps. Where this is done, the choice of the small map area and size must be such that the unavoidable effect of small misalignments between does not lead to significant numbers of additional grain boundaries at the joins between maps.

If possible, a large area should be mapped with automated routines that stitch together multiple smaller maps. Where this is done, the choice of the small map area and size must be such that the unavoidable effect of small misalignments between does not lead to significant numbers of additional grain boundaries at the joins between maps.

3.2 Grain size measurement

In many cases grain sizes from EBSD maps are reported as the diameters of circles of area equal to that of the grains – the circle equivalent diameter or Dceq. In sections where the grains are equiaxed (Figure 2), this may well be appropriate, but with elongated grains other options such as linear intercept measurements need to be considered and descriptors of shapes also need to be used.

Before considering these other descriptors it is worth examining the use of the standard circle equivalent diameter to see how it can discriminate between two Ni superalloys shown below in Figure 9 at the same magnification. By eye, the overall grain shape suggests a similarity in structure but Sample 1 in Figure 9a has a smaller grain size than Sample 2 in Figure 9b. Figure 9b is the same as that shown in Figure 8 and is taken from the middle of the sample described by Figures 3-7.

a) b)

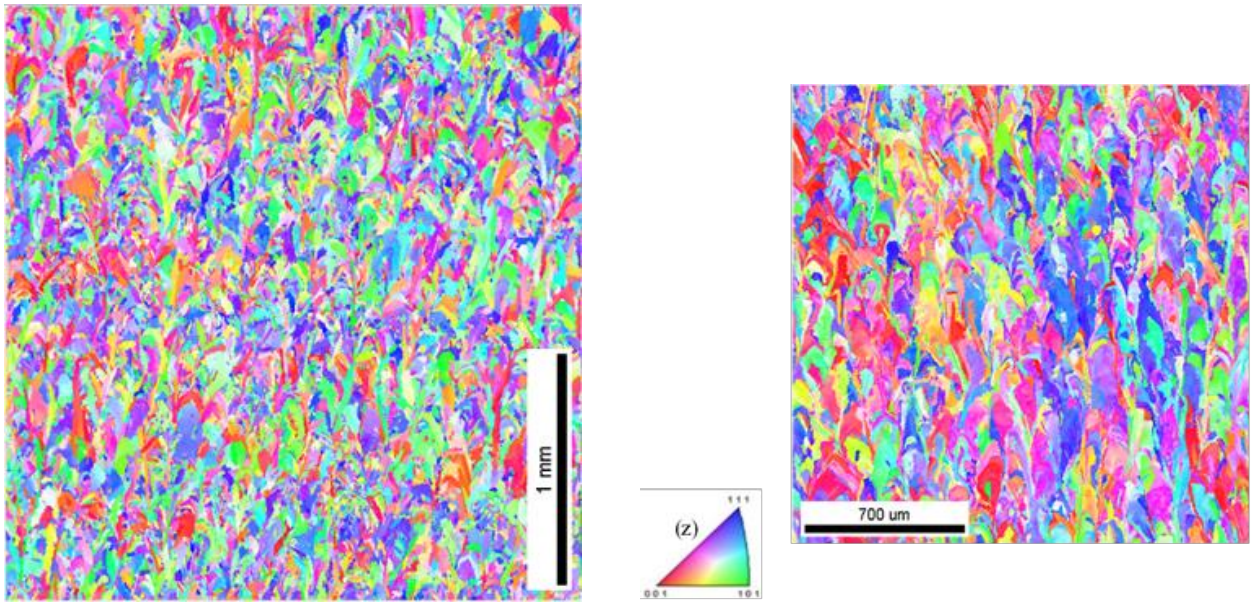

***Figure 9**. Ni superalloy samples shown at the same magnification: a) Sample1. Mapped with 5 µm step size, 5985 grains ≥10 pixels in area, b) Sample 2. Mapped with 3 µm step size, 2718 grains >= ≥10 pixels in area.*

3.2.1 Mean grain size calculation

It is possible to determine a mean grain size diameter from several different calculations.

$$\overline{D_{ceq(n)}} = \frac{\sum_{i=0}^{n} D_{ceq(i)}}{n} \quad (1)$$

$$\overline{D_{ceq(A)}} = \sqrt{(4\overline{A}/\pi)} \quad \text{(where } \overline{A} = \frac{\sum_{i=0}^{n} A_i}{n}\text{)} \quad (2)$$

$$\overline{D(A)_{ceq}} = \frac{\sum_{i=0}^{n}(D_{ceq(i)}A_i)}{\sum_{i=0}^{n} A_i} \quad (3)$$

Equation 1 gives the commonly quoted number average diameter which is simply the sum of all the individually calculated circle equivalent diameter divided by the number of grains. Equation 2 calculates the number average area instead, and then converts this average area to a circle equivalent diameter; for equiaxed materials this can be related to the mean lineal intercept (stereologically the same in both 2D and 3D measurements) via the Tomkeieff relationship [15] . Equation 3 calculates the area weighted mean diameter and thus gives greater emphasis to the largest grains. Table 1 summarises the mean values calculated by these three methods for the two maps shown in Figure 9.

Table 1. *Average Grain Size* (D_{ceq}) *values (all in µm) for Samples 1 and 2 in Figure 9.*

	Number average Diameter $D_{ceq(n)}$	**Mean Area Diameter $D_{ceq(A)}$**	**Area weighted Diameter $D(A)_{ceq}$**
Sample 1, 10 pixel min (16.6 µm)	29.4	32.8	47.7
Sample 1, 5 pixel minimum (11.7 µm)	23.3	27.2	44.5
Sample 2 (Figure 9b) 10 pix (10.7 µm)	29.4	39.2	81.9
Sample 2, (whole area of Figure 3)	31.0	40.5	85.7

Comparing the number average diameter for the two samples would suggest little difference between them. It can also be seen that the map acquisition and analysis parameters have an influence on the mean values. The first row for each sample shows the values when all regions of less than 10 pixels are ignored, but because the larger map of Sample 1 was produced with a 5 µm pixel size rather than 3 µm, this eliminates grains of a size that are analysed for Sample 2. If only regions of less than 5 pixels are included for Sample 1 so calculations cover approximately the same size range for both, the data will now include grains that will not be accurately measured; it does however reduce the number average grain size of Sample 1 by 20%.

The effect of the pixel size is much reduced if the mean area diameter is calculated and Sample 1 clearly has a mean size about 20% less than Sample 2. If however the area weighted diameter is calculated then the effect of pixel size is reduced still further and a difference in mean grain size between the samples of 40% can be reported.

3.2.2 Grain size distributions

3.2.2.1 Histograms

A mean grain size value cannot fully describe a sample with a wide range of sizes. Typically, histograms are used to illustrate the size distribution and Figure 10 shows examples of these for Samples 1 and 2 in Figure 9; Figure 10a) shows the distribution of sizes by the number of grains within each 10 µm range, and Figure 10b the distribution by area fraction. As with the area weighted mean values, the area weighted histogram illustrates the difference between the two samples much more clearly than the number fraction plot.

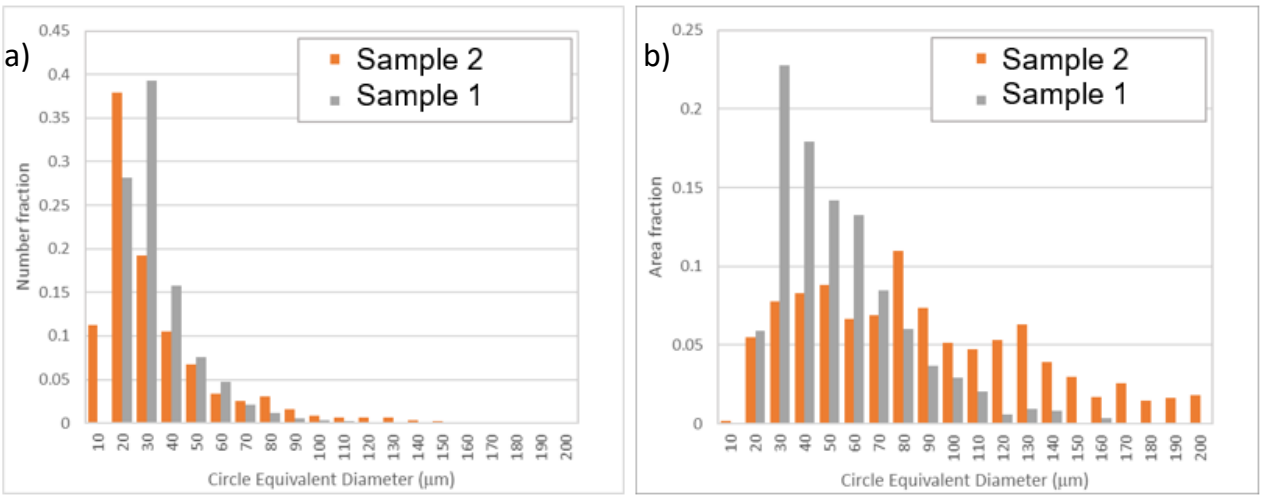

Figure 10. *Histograms of a) number fraction and b) area fraction for maps of Samples 1 and 2 shown in Figure 9.*

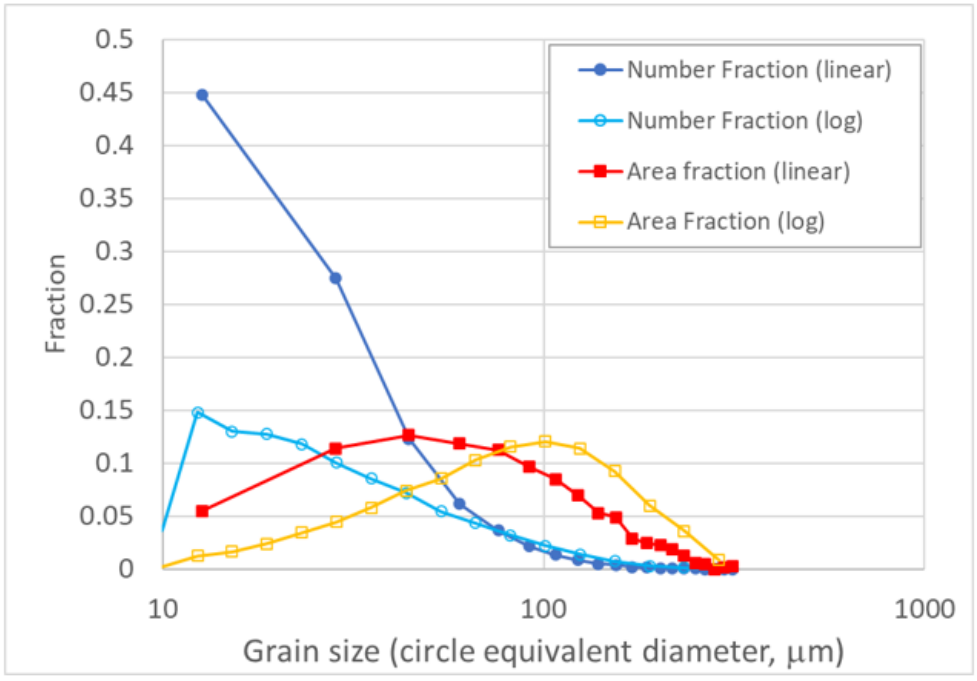

Figure 11. *Histograms of the number and area fraction grain size distribution of Sample 1, measured from the same map but plotted with the equal width size divisions determined from linear and log scales.*

In addition to being dependent on the choice of scaling by number or area fraction, histograms are, also dependent upon how the size data is binned. Figure 11 shows an example of four different ways of plotting the same grain size distribution; in addition to plotting the number and area fractions of the previously used subdivision into equal 10 µm ranges, the result of subdividing to give equal widths on a log scale are shown. The log scale binning increases the number of ranges at the lower size end and reduces them at larger values, shifting the distribution down and to the right.

3.2.2.2 Cumulative Distribution Plots

An alternative to histograms is to plot all the data in a cumulative curve, ordering the data for each grain by increasing size and calculating a value for each set of grain data between 0 and 1 reflecting its position in this ordered list. This value can either reflect simply the numerical position of the grain in the list (a cumulative frequency), or the area as a fraction of the total area of the grain plus all smaller grains (a cumulative area fraction).

Figure 12 shows how such cumulative distribution curves for samples 1 and 2 clearly discriminate between the two samples. A greater separation is seen for the area fraction curves, and it can be seen the median values when the fraction = 0.5 are close to the mean values shown previously. The difference in the maximum grain size is also more clearly visible in the area fraction curves, while the effect of the choice of minimum grain size can be seen in both, but particularly the cumulative frequency curve. The curves can also be used to determine easily values such as d10 and d90, the diameters at which 10% and 90% of the number or area fraction (which obviously must be specified) are reached.

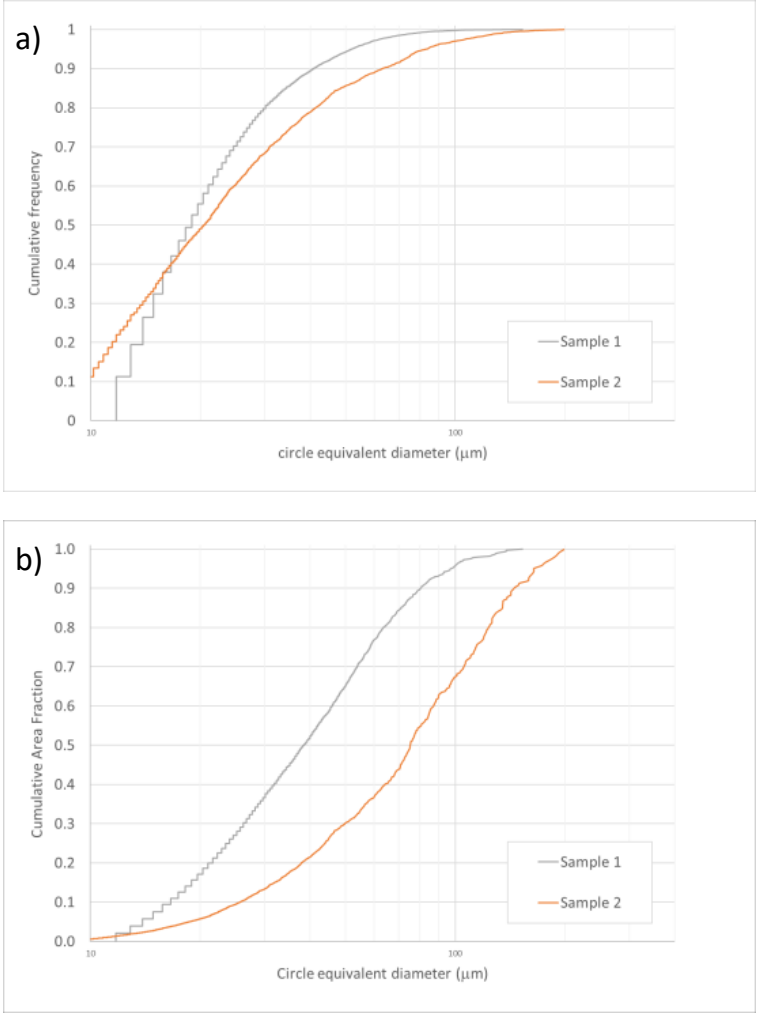

Figure 12. *Cumulative frequency plots of the grain size distributions from Samples 1 and 2. a) number fraction and b) area fraction*

An alternative cumulative plot is to assume the sizes are (log) normally distributed and convert the cumulative number to a value that represents its position on the distribution curve, shown below in Figure 13 as the number of standard deviations from the mean. Although arguments for a log normal distribution have been derived for equiaxed materials [16,17] and not the elongated structures seen in the example AM materials used here, the approximation to the expected straight line over a significant fraction of the distribution is still evident in Figure 12a is still clear for Samples 1 and 2. The two samples can clearly be distinguished by their different slopes and intercepts on the X axis and the different maximum sizes of the two samples are also obvious in Figure 12a. The tails to smaller sizes are clearly affected by the minimum size measured. There is less reason to suppose the area would be log normally distributed, but this data too can be plotted, as shown in Figure 12b.

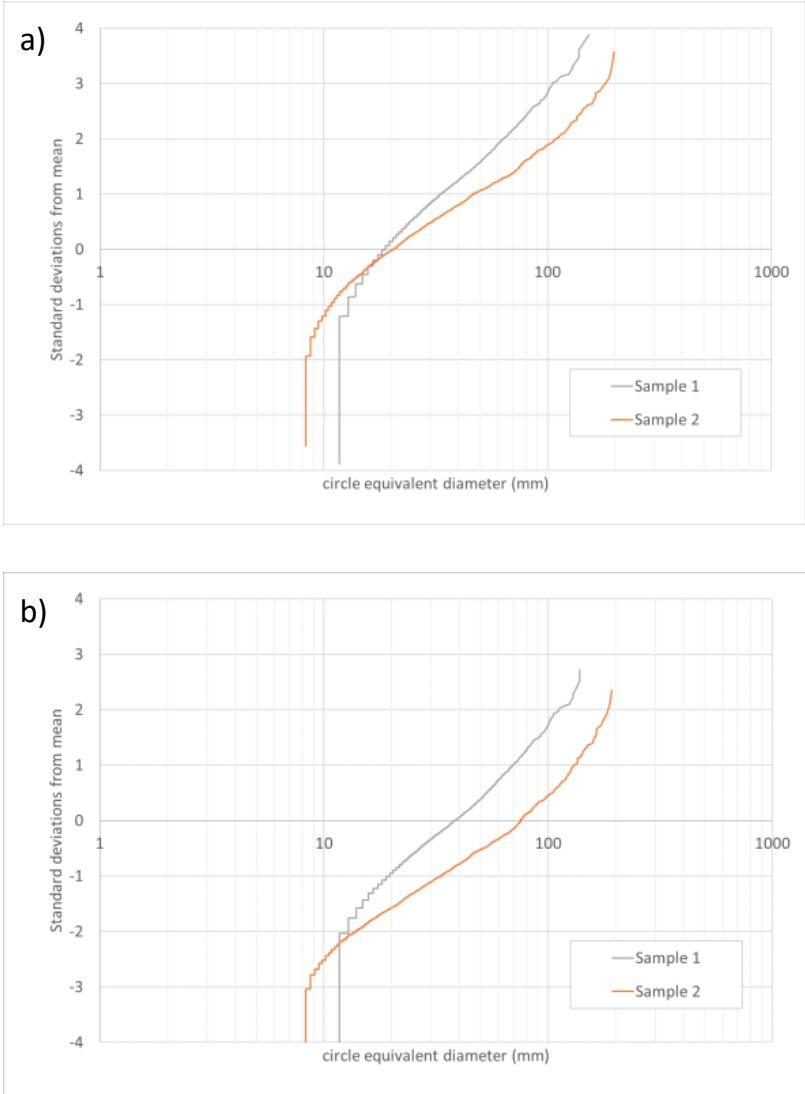

Figure 13. *Cumulative frequency plots of the grain size distributions of Samples 1 and 2 for a) number and b) area fraction; a log normal distribution of the values would lead to a straight line.*

3.3 Other size parameters

For the elongated grains of the examples shown in the previous section, the circle equivalent diameter is possibly not the most appropriate parameter to measure. Possibilities include the use of:

- Linear intercept measurements parallel and perpendicular to the growth direction
- Maximum and minimum Feret diameters
- Ellipse fitting to determine major and minor axes
- Calculation of the aspect ratio from the above

Linear intercept measurements are perhaps the most straightforward to make and yet are often not clearly implemented (if at all) in commercial EBSD software.

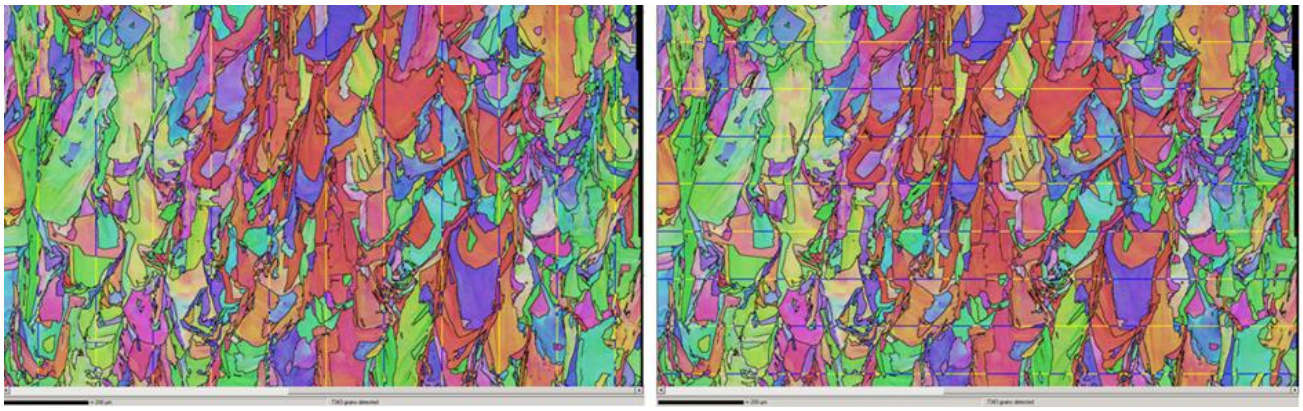

Figure 14. *Selected region of map from Sample 2 displaying linear intercept measurement with individual intercepts shown and saved for analysis.*

The alignment of the dimensions can be directly related to the sample axes but, like circle equivalent diameter values, care must be taken to ensure pixel size and the minimum intercept lengths used are documented and are equivalent when comparisons are made between data sets. Area weighted average linear intercepts (by assuming each intercept is equivalent to the grain diameter) again reduce dependence on pixels size and minimum lengths.

The advantage of the other parameters listed above are that they derive from all the grains in the data set and not just a sample. However, a very significant factor to beware of when publishing the data or using any of the above to compare datasets is understanding exactly how each feature is defined. The Maximum Feret diameter is relatively straightforward, being the longest length that could be contained by the jaws of a caliper. The Minimum Feret diameter should then simply be the smallest length; however, the shortest distance at right angles to the maximum Feret diameter is often reported, although this should then be called the Minimum Orthogonal Feret diameter.

Ellipse fitting is also commonly used to give a maximum and minimum dimension from the major and minor axes of the fitted ellipse, but there are multiple ways of fitting an ellipse to a general shape which will produce different results. Possible methods include:

- A least squares approach to minimise the distance between the grain edges and a fitted ellipse [18]
- Use of a Feret diameter to define the major axis and then averaging the grain boundary distance to the major axis along its length
- Use of a Feret diameter as before and then calculating the minor axis to give the same area as the grain itself
- A Covariance best fit method constrained by the actual area of the grain [19]

Clearly, whichever method is used should be stated as results can vary significantly between the calculations.

For calculation of the Aspect Ratio, again, the ellipse fitting calculation chosen must be specified as it obviously affects the ratio of the major to minor axis. This Aspect ratio is also sometimes defined as major/minor axis, giving values ≥ 1 so the more elongated the larger the value, or conversely, minor/major giving values ≤1 and smaller values indicate a higher aspect ratio.

As an example, Sample 2 was mapped and analysed with software from two different vendors and the data output from the two is shown in Table 2.

Table 2. *Effect of different software on reported shape parameters. (Data from mapping > 4000 grains from the same sample. All dimensions in mm. Minimum Feret diameter not reported by Software 1)*

	Diameter d_{ceq}	**Major axis**	**Max. Feret Ø**	**Minor axis**	**Min. Feret Ø**	**Aspect ratio**
Software 1	88.6	156.8	198.9	52.5	N.R.	3.3
Software 2	85.7	95.9	191.8	21.8	53.0	0.27

The areas chosen and indeed the pixels sizes were not identical so the results would not be expected to be identical. In fact, the area weighted mean circle equivalent diameter and Maximum Feret diameters are very similar, each differing by about 3.5%. One reason for the large difference in major axis values is that the second vendor reports the radius of the fitted ellipse (it can be seen this is half the Max. Feret diameter), while the first reports the diameter of the ellipse. Even after allowing for this, the values differ by about 20%, which suggests the first has been calculated by a best fit approach. The aspect ratio is presumably reported by the two software versions as the inverse of the other, i.e. minimum/maximum or maximum/minimum of the ellipse diameters.

Ellipticity (and averages thereof) is another parameter that can be reported, but a range of definitions for this parameter exist, including

$$\epsilon = \frac{a}{b} \qquad \varepsilon = \frac{a-b}{a} \qquad \text{and} \qquad \varepsilon = \frac{a^2-b^2}{a^2}$$

Where the first one is clearly the same as one of the reported aspect ratios. If it is used this parameter needs to be very carefully defined along with the method calculation of the ellipse parameters.

Circularity can also be measured and reported, but as this requires the measurement of the grain perimeter, the effect of the map step/pixel size can alter the calculation significantly so comparisons can only be made between maps of a similar step size.

3.4 Summary

- If measurements are to be taken from a map, ensure that it covers sufficiently large an area, especially in the case of elongated grains
- For large area/low magnification maps, consider stitching smaller areas acquired at higher magnifications to avoid edge distortions
- For many AM structures, use of a weighted average will give more consistent results with less dependence on the effect of step size and map quality
- Cumulative distribution graphs may illustrate differences between materials more clearly than histograms
- Parameters such as Feret Diameters, Linear Intercept or Ellipse fitted axes may give more useful information for non-equiaxed grains. However:
- Ensure the definition used to measure the parameter is known, or at a minimum the software used is reported to enable comparisons.

Chapter 4

Visualisation of variation

4.1 Colour scale maps

Having established some of the characteristic parameters of AM microstructures that can be quantified and averaged over an entire map or sample, it is also worth considering how best to understand the uniformity or otherwise of these parameters across a large region. AM microstructures are determined by the melting of the powder layers and subsequent solidification. Local variations in heat flow caused by changes in geometry, powder layer deposition or input power and scan patterns can therefore lead to local variations in solidification rates and thus microstructure.

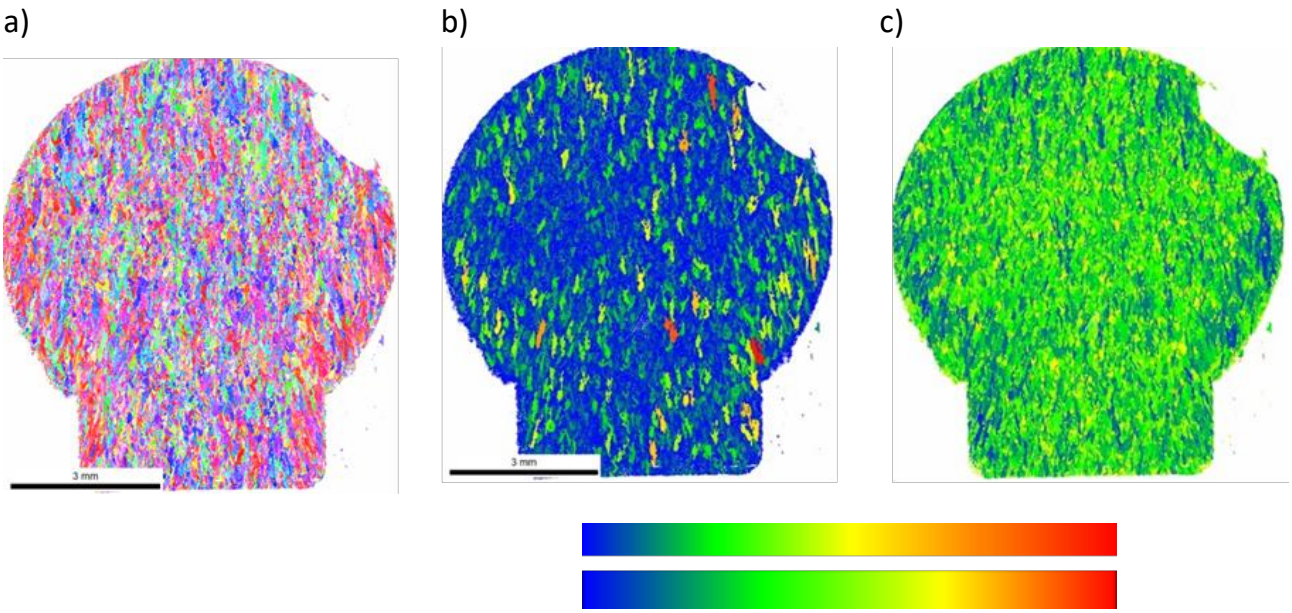

Figure 15. *a) IPF(z) orientation colour scale map shown previously b) circle equivalent diameter grain size and c) aspect ratio maps of the same sample. Maps b) and c) both plotted using the uppermost default rainbow colour scale with ranges respectively of 5 to 330 µm and 0.04 to 1. The lower rainbow colour scale is the default scale for a second EBSD software program and is shown to illustrate the (undefined) differences in the ranges they will emphasise.*

The IPF-Z orientation map shown previously in Figure 4 is shown in Figure 15a), alongside maps of the grain size and aspect ratio plotted with commonly used rainbow colour scales spanning the minimum to maximum values in each map. Both suggest a tendency to larger more elongated grains around the periphery of the sample, particularly where there is an increase in sample width as the circular profile develops. However, these trends are not particularly clear, and it is difficult to describe them simply or to enable a comparison between them.

Before going on to illustrate other possibilities for revealing variation in structure, reference should be made to a number of general issues with default scales provided with software:

a) The transition between colours may at first glance appear to be the same for a given scheme, but as Figure 15 shows, when laid side by side, the scales can be very different in positioning and gradients of the transitions.

b) There are often flat zones in colour scales which means that within these zones no variation will be detected. This may be useful if only one part of the distribution is of interest, but equally may hide variations.

The perceptual contrast between positions on a scale are often uneven; the perceived variation seen by eye is dependent not just on the colour value (hue, given by e.g. RGB values) but also on the saturation (colour intensity), lightness and brightness.

More details on colour scales and the perception of differences may be found in [20]. The preceding does not mean that default scales are not useful, since if always used they will allow accurate comparisons between maps to be made. Conversely, scales can be difficult to define simply so the ability to make comparisons is impossible if they are adjusted without clear records. Figure 16 shows an example where the same basic two colour scale is used, but the transition and gradient has been altered to give a completely different impression of the variation in aspect ratio across the sample.

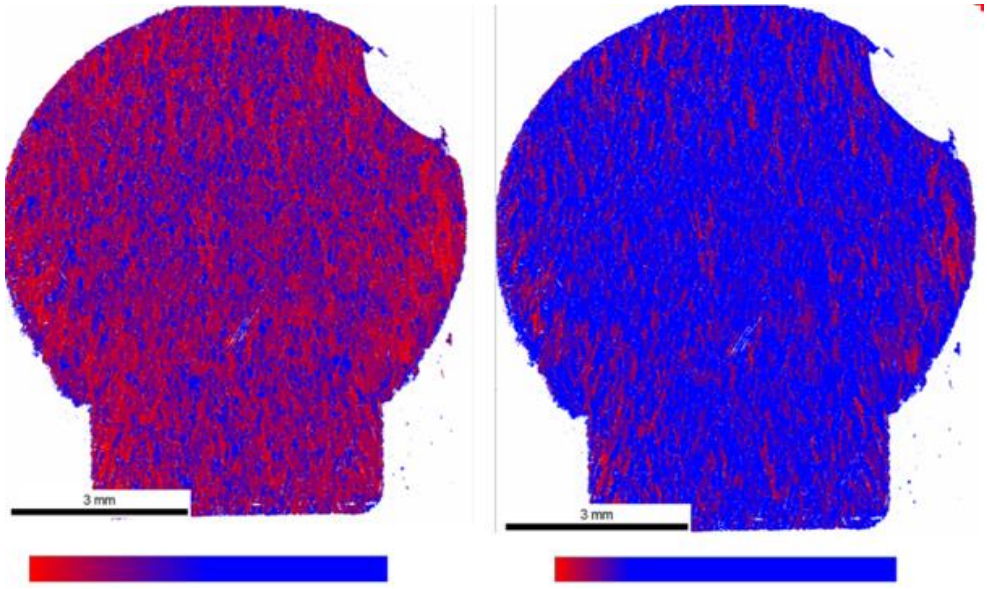

Figure 16. *Repeat of the aspect ratio maps shown in Figure 15 c) with the same red-blue colour scale covering the range 0.04-0.5, but with a different point of transition and gradient between them.*

If, however, a fixed colour scale is chosen (commonly the user has no control of the scale), variation in what is seen still possible simply by altering the maximum and minimum values that correspond to the full scale. This is effective when the full range is distorted by a few extremes. Reducing the scale range of Figure 16c in Figure 17a shows how the high aspect ratio grains seen in blue original appear less obvious in the latter, and even after simply inverting the colour scale. At first glance it may not be appreciated that all three maps show

the same data. Red-green colours may also not be good as it is the most common form of colour blindness (≈1 in 12 men).

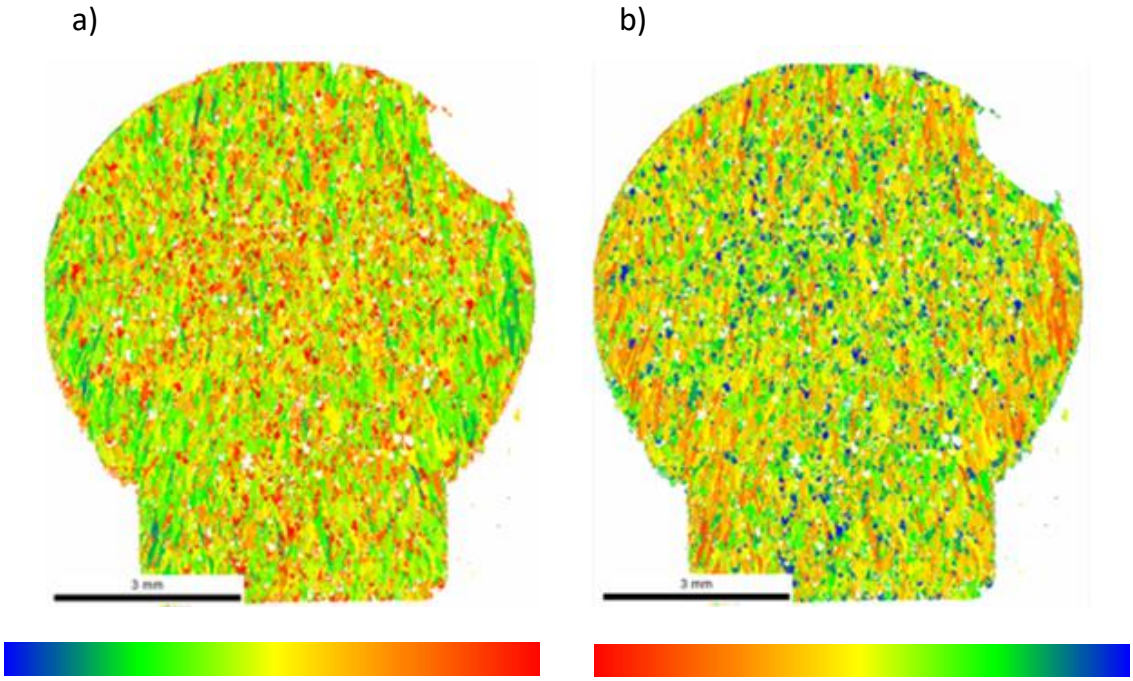

Figure 17. *Rainbow colour scale used to show the aspect ratio variation but with scale (0.04-0.5) reversed between a) and b).*

Binary colour scales such as those shown in the preceding Figure 16 may therefore be easier to interpret, particularly when primarily the extreme values such as the largest or most elongated grains.

4.2 Use of grey scale maps

Possibly the best approach for such circumstances is to use a grey scale with a linear gradient between black and white, and to use the scale limits to highlight the required information. Figure 18 a) and b) show examples of this for the grain size and aspect ratio maps.

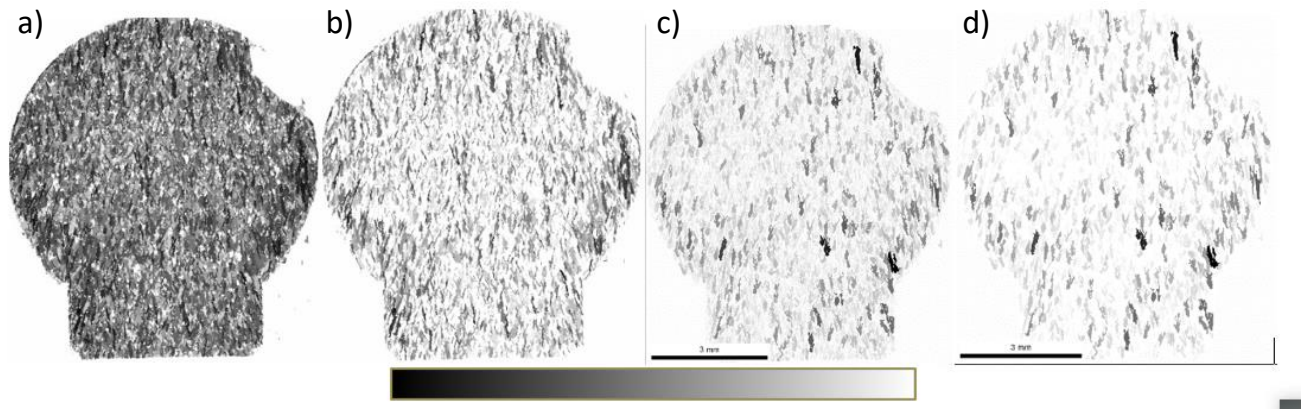

***Figure 18**. Grey scale maps showing a) Aspect ratios (0.04-0.5) and b) Aspect ratios 0.04-0.25: c) Circle equivalent diameter grain size (30-321 µm) and d) as c) but size range 100-321 µm.*

The grey scale shown in Figure 18 is the default scale produced by a manufacturer's EBSD software and it can be verified readily that it has a linear transition from black (0) to white (255) on an 8 bit greyscale. However, when the actual greyscale values plotted on an example map are compared with the corresponding grain size (circle equivalent diameter), it is found that in plotting the map, a gamma correction has been applied which accentuates the variation between larger grains in the map and reduces it for the smaller grains (Figure 19).

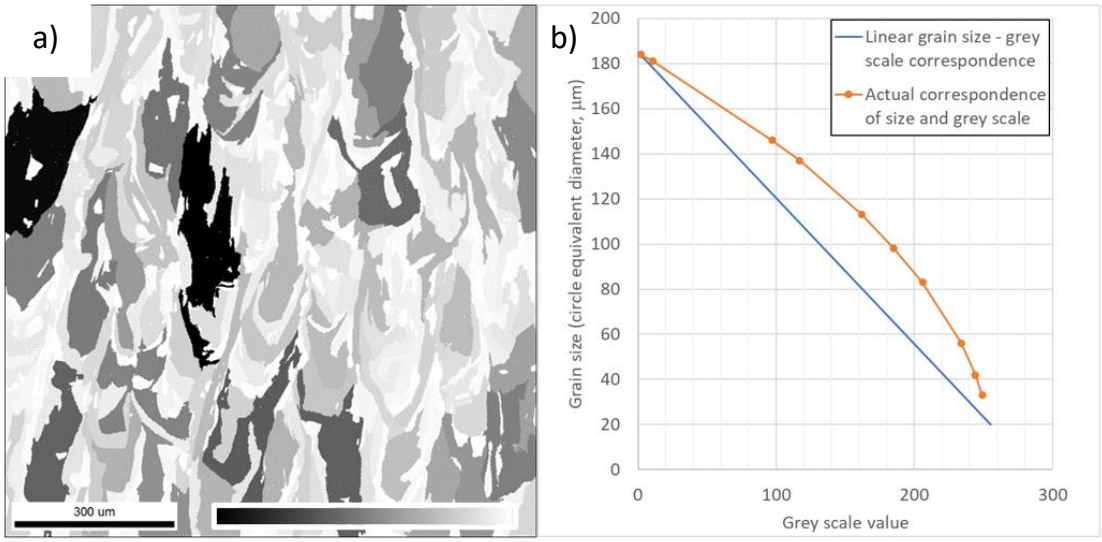

***Figure 19.** a) Enlargement of a region of the sample shown in Figure 18, with the reported grey scale shown and b) a graph of the grey scale showing linear decrease of reported grey scale (blue line) compared with actual grey scale-grain size correspondences measured for a range of grain sizes.*

The use of grey scale maps also allows for the rapid assessment of variability with position. Using an image analysis program such as ImageJ, the brightness profile of a broad line drawn across the sample at any given position will give a plot of the average grain size. This avoids the need to divide the map data into subsets and overcomes the difficulties of the subsequent subsets only including partial data for the grains intersected by the subset borders. Although the grey scales do not give the grain size immediately (and as plotted will give an inverted view

of the size if white = 255), a simple linear conversion can produce the graphs shown below in Figure 20 c) and d). However, the linear correction gives a mean value lower than the true value because of the (undefined) gamma correction noted in Figure 19. With further correction for this gamma correction, the values should correspond to an area weighted mean value. Even without correction, these graphs clearly quantify trends in average values with lateral and vertical positions, and the degree of local uniformity which otherwise would be difficult to describe.

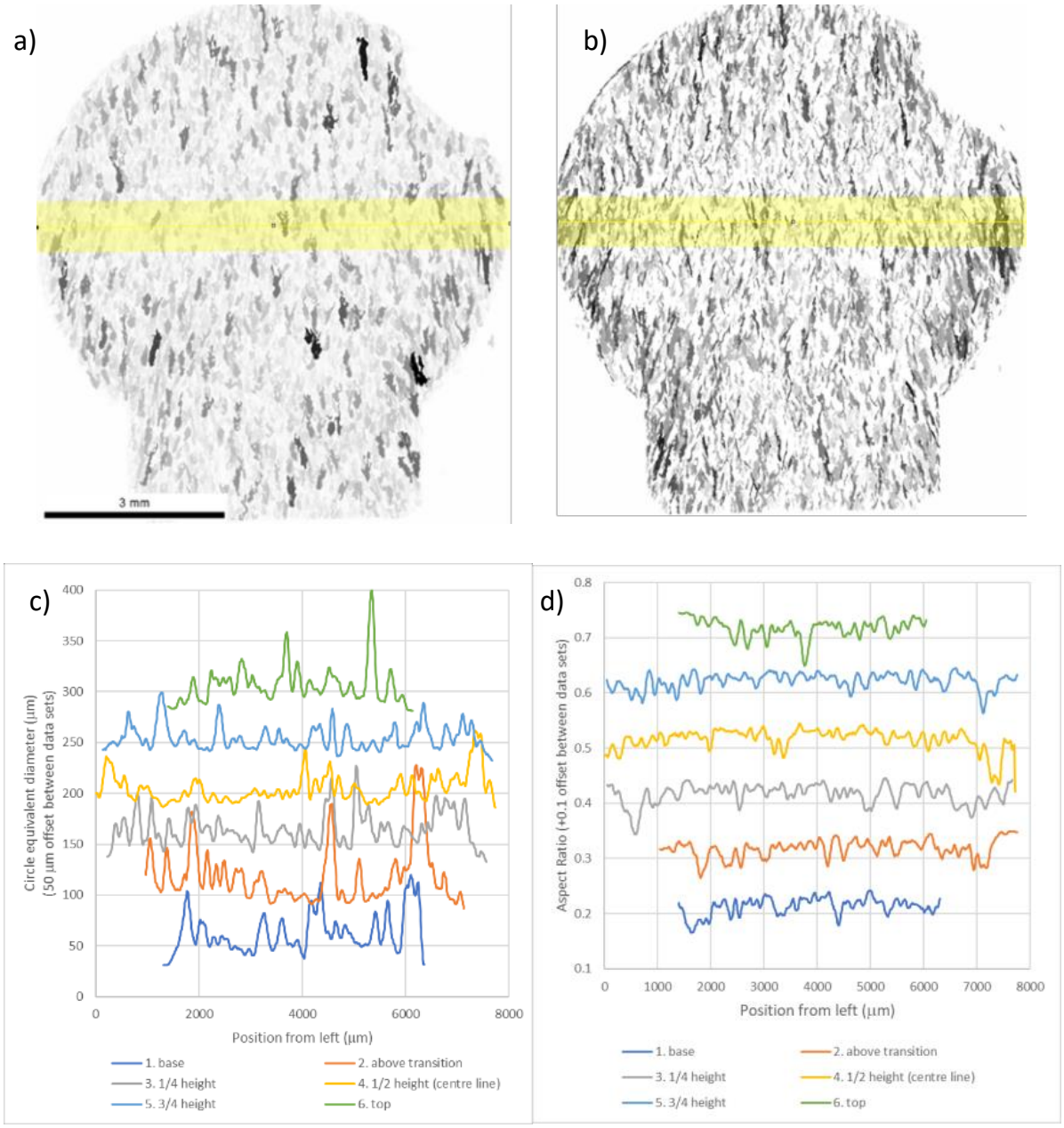

Figure 20. *a) Grain size (30 – 321 µm) and b) aspect ratio (0.04 – 0.25) grey scale maps showing 100 pixel wide (≈0.8 mm) bands on maps reduced to 1024 pixels height for measurement of features. c) 25 point moving average graphs of grey scale converted to circle equivalent diameter assuming a linear transformation, d) as c) but for aspect ratio.*

4.3 Summary

- Colour and grey scale maps can be used to show the uniformity or otherwise of microstructural parameters over large areas
- Scales which have transitions between colours or grey levels can appear similar but need to be carefully defined so the similarity can be established before comparisons are made.
- Even when a map's colour (grey) scale is shown, the actual correspondence between the map parameter and the scale may be distorted
- Image analysis of grey scale maps can be used as a quick and simple way to plot variation with position in large scale maps

This page was intentionally left blank

References

1. M-S.Pham, B Dovgyy, P.A. Hooper, C.M.Gourlay and A.Piglione, The role of side-branching in microstructure development in laser powder-bed fusion, Nature Communications, (2020) 11:749, https://doi.org/10.1038/s41467-020-14453-3

2. A.Piglione, B.Dovgyy, C.Liu, C.M.Gourlay, P.A. Hooper and M.S. Pham, Printability and microstructure of the CoCrFeMnNi high-entropy alloy fabricated by laser powder bed fusion, Materials Letters 224 (2018) 22–25

3. D.J.Rowenhorst and R.W.Fonda, Combining EBSD with Serial Sectioning for the 3D Analysis of Materials, Microsc. Microanal. 25 (Suppl 2), (2019), doi:10.1017/S1431927619002460

4. A.T.Polonsky, C.A.Lang, K.G.Kvilekval, M.I.Latypov, ·M.P.Echlin, B. S. Manjunath and T.M.Pollock, Three-dimensional Analysis and Reconstruction of Additively Manufactured Materials in the Cloud-Based BisQue Infrastructure, Integrating Mater. and Manuf. Innovation (2019) 8:37–51, https://doi.org/10.1007/s40192-019-00126-7

5. S.Gorsse, C.Hutchinson, M.Gouné and R.Banerjee, Additive manufacturing of metals: a brief review of the characteristic microstructures and properties of steels, Ti-6Al-4V and high-entropy alloys, Science and Technology of Advanced Materials, 18:1, 584-610, (2017), DOI: 10.1080/14686996.2017.1361305

6. Y. M.Wang et al., Additively manufactured hierarchical stainless steels with high strength and ductility Nature Materials, 17, 63-73, (2018), DOI: 10.1038/NMAT5021.

7. V.A.Popovich, E.V.Borisov, A.A.Popovich, V.Sh.Sufiiarov, D.V.Masaylo and L. Alzina, Functionally graded Inconel 718 processed by additive manufacturing: Crystallographic texture, anisotropy of microstructure and mechanical properties, Materials and Design ,114 (2017) 441–449

8. T.B.Britton, https://www.youtube.com/watch?v=BTx16E7YUbs

9. A. J. Schwartz, M. Kumar, B. L. Adams, and D. P. Field, Electron Backscatter Diffraction in Materials Science, (Springer, New York, 2009),

10. T.B. Britton, J. Jiang, Y. Guob, A. Vilalta-Clemente, D.Wallis, L.N. Hansen, A. Winkelmann, A.J. Wilkinson Tutorial: Crystal orientations and EBSD — Or which way is up? Materials Characterization 117 (2016) 113–126

11. J.K.Mason and CA.Schuh Representations of Texture in [9]

12. V.Randle and O.Engler, Texture Analysis, (2000) CRC Press, Boca Raton

13. ISO 13067:2020 Microbeam Analysis – Electron backscatter diffraction – Measurement of Average Grain Size, https://www.iso.org/obp/ui#iso:std:iso:13067:ed-2:v1:en

14. G.Nolze, Image distortions in SEM and their influences on EBSD, Ultramicroscopy 107 Pages 172-183

15. Y. Takayama, N. Furushiro, T. Tozawa, H. Kato and S. Hori. A significant method for estimation of the grain size of polycrystalline materials. Mat. Trans. JIM, 32(3), 1991, 214-221.

16. M.Fátima , .A.Fortes, Grain size distribution: The lognormal and the gamma distribution functions, Scripta Metallurgica 22, 1988, 35-40

17. Y.A. Coutinho, S.C.K. Rooney and E.J. Payton, Analysis of EBSD Grain Size Measurements Using Microstructure Simulations…, Metal. Mater. Trans.A, 48A, 2375-2395 (2017) doi: 10.1007/s11661-017-4031-z

18. S. Biggin and D.Dingley, A least squares approach to minimise the distance between the grain edges and a fitted ellipse, J. Appl. Crystallography (1977) 10,376-385

19. K.F.Mulchrone and K.R.Choudhury. Fitting an ellipse to an arbitrary shape: Implications for strain analysis. J.Structural Geol., 26, 143-153, 2004

20. P.Kovesi; Good Colour Maps: How to Design Them. arXiv:1509.03700v1 [cs.GR] 12 Sep 2015 and https://colorcet.com/userguide/index.html